Chemistry & Biology
Article

Profiling the Sulfation Specificities of Glycosaminoglycan Interactions with Growth Factors and Chemotactic Proteins Using Microarrays

Eric L. Shipp[1] and Linda C. Hsieh-Wilson[1,*]
[1] Division of Chemistry and Chemical Engineering and Howard Hughes Medical Institute, California Institute of Technology, 1200 E. California Boulevard, Pasadena, CA 91125, USA
*Correspondence: lhw@caltech.edu
DOI 10.1016/j.chembiol.2006.12.009

SUMMARY

We report a carbohydrate microarray-based approach for the rapid, facile analysis of glycosaminoglycan-protein interactions. The key structural determinants responsible for protein binding, such as sulfate groups that participate in the interactions, were elucidated. Specificities were also readily compared across protein families or functional classes, and comparisons among glycosaminoglycan subclasses provided a more comprehensive understanding of protein specificity. To validate the approach, we showed that fibroblast growth factor family members have distinct sulfation preferences. We also demonstrated that heparan sulfate and chondroitin sulfate interact in a sulfation-dependent manner with various axon guidance proteins, including slit2, netrin1, ephrinA1, ephrinA5, and semaphorin5B. We anticipate that these microarrays will accelerate the discovery of glycosaminoglycan-binding proteins and provide a deeper understanding of their roles in regulating diverse biological processes.

INTRODUCTION

Heparin and heparan sulfate (HS) glycosaminoglycans play important roles in many physiological and pathological processes such as cell growth, viral invasion, angiogenesis, and cancer. The chemical diversity of HS, represented by varied stereochemistries and sulfation patterns, is believed to have important functional consequences, enabling a large number of protein-binding motifs to be generated from a relatively simple scaffold [1, 2]. Indeed, glycosaminoglycans have been shown to interact with a wide range of proteins, including growth factors, metalloproteinases, chemokines, and pathogenic proteins [1, 2]. Despite intense study, the precise sequences involved in protein recognition are understood only in a few cases [3–5]. Elucidating the sulfation specificities of the growing number of HS-binding proteins in the genome will be critical for understanding the structure-activity relationships of glycosaminoglycans and the molecular mechanisms underlying important biological processes.

Several powerful methods have been developed to study glycosaminoglycan-protein interactions [6]. Typically, small oligosaccharide libraries are created from naturally occurring polysaccharides by heparinase treatment and, in some cases, chemical desulfation followed by resulfation with various sulfotransferase enzymes [6–8]. The oligosaccharides are then radiolabeled, and HS-protein interactions are evaluated by affinity chromatography or electrophoretic mobility shift assays [7, 9–11]. Alternatively, indirect competition assays have been used to determine the sulfation specificities of proteins by using free heparin of varying sulfation patterns to disrupt the binding of proteins to immobilized heparin [6, 12]. Mass spectrometry has been applied recently to characterize the binding of HS to certain proteins, such as chemokine ligand 2 and fibroblast growth factor-2 (FGF2) [13, 14]. Finally, surface plasmon resonance and isothermal calorimetry have been exploited to provide quantitative information about HS-protein interactions [15–17]. Although effective, none of these methods is ideally suited to the direct, high-throughput analysis of glycosaminoglycan-protein interactions. Existing approaches are generally labor intensive, require specialized equipment, consume significant amounts of carbohydrate or protein, and/or involve handling of expensive radioactive materials. Given the large number of binding partners and diverse glycosaminoglycan structures, new tools are needed to study glycosaminoglycan-protein interactions: specifically, to examine systematically how the sulfation patterns of HS direct its interactions with proteins, to identify biologically active motifs more rapidly, and to look globally across protein families and glycosaminoglycan classes to understand the role of specific interactions in physiological processes.

Recently, we and others have developed carbohydrate microarrays for the high-throughput analysis of carbohydrate-protein interactions [18–31]. The miniature array format permits detection of multiple binding events simultaneously and requires minimal amounts of carbohydrate

and protein. Several systems have been used to profile a wide range of carbohydrate-binding proteins, including growth factors and cytokines [22–25, 30], lectins [24, 26, 28], antibodies [20, 27], and cell receptors [21, 24]. In a few cases, microarrays of chondroitin sulfate (CS) and HS oligosaccharides have been demonstrated to be powerful tools for studying the binding of proteins to specific sulfation sequences [22, 23, 25].

Here, we report a facile, microarray-based approach that enables rapid interrogation of any protein of interest for binding to various glycosaminoglycan sulfation patterns and classes. The key structural determinants responsible for protein binding, such as sulfate groups that participate in the interaction, are elucidated. Moreover, sulfation specificities can be readily compared across large families or functional classes of proteins. As the approach is amenable to all glycosaminoglycan subtypes, direct comparisons of HS, CS, keratan sulfate (KS), and other classes are possible, providing a more comprehensive understanding of the specificity of proteins for various glycosaminoglycans. In this study, we validate the approach by showing that members of the FGF family have distinct sulfation preferences, consistent with earlier structural and biochemical studies, and we further extend those findings by identifying the sulfation requirements for two previously uncharacterized members, FGF16 and FGF17. In addition, we illustrate the power of glycosaminoglycan microarrays to rapidly provide new information regarding the interactions and functions of HS by demonstrating that HS interacts with a number of axon guidance proteins such as slit, netrin, ephrin, and semaphorin. Sulfation of HS is shown to modulate the specificity of those interactions and may provide a means to fine tune the localization and activity of chemotactic proteins during neuronal development.

RESULTS AND DISCUSSION

Development of Glycosaminoglycan Microarrays

In designing the microarrays, we sought to develop a rapid, convenient approach that would not require specialized expertise in carbohydrate or surface chemistry. As such, we chose a flexible, noncovalent strategy for attachment of glycosaminoglycans to poly-L-lysine (PLL)-coated slides. CS oligosaccharides have previously been immobilized noncovalently on nitrocellulose membranes, but the approach required synthesis of a neoglycolipid conjugate for each oligosaccharide [27]. We wanted to circumvent these derivatization steps and exploit the high-throughput robotic printing and fluorescence scanning technology used for microarrays. Based on strong precedent with other charged glycans [30, 31] and DNA [32, 33], we reasoned that anionic glycosaminoglycans might adhere to PLL-coated slides while maintaining the ability to interact with proteins.

To validate the approach, we first examined whether polysaccharides of differing sulfation patterns adhere uniformly to PLL-coated surfaces. Heparin polysaccharides (MW of ~13,000) varying in the number and position of sulfate groups were labeled at the reducing end with 5-(((2-(carbohydrazino)methyl)-thio)acetyl)aminofluorescein in the presence of sodium cyanoborohydride. Specifically, we used polysaccharides that had been chemically desulfated at key positions: 2-*O*-desulfated heparin in which the 2-*O*-sulfate groups of uronic acid had been removed (2-deO), 6-*O*-desulfated heparin wherein the 6-*O*-sulfate groups of glucosamine had been removed (6-deO), fully *N*-acetylated heparin in which the amino groups of glucosamine were desulfated and *N*-acetylated (N-Ac), and fully *O*-desulfated heparin (deO) (Figure 1). These naturally derived polysaccharides were chosen because previous studies have exploited such preparations to understand glycosaminoglycan-protein interactions [12, 34–36]. Moreover, the use of HS isolated from natural sources would enable profiling of protein-binding patterns to glycosaminoglycans in different cell types, organs, or developmental stages. Equal concentrations of the polysaccharide-fluorescein conjugates were manually spotted onto PLL slides, and after washing with 0.5 M NaCl and PBS, the fluorescence intensity at 530 nm was measured relative to an unconjugated fluorescein control. Importantly, we found that the derivatives adhered uniformly to the slide surface irrespective of the sulfation pattern (Figure 2A). Approximately 86% of the polysaccharide attached to the surface in each case, indicating efficient and uniform immobilization of the polysaccharides. Attachment of the carbohydrate was stable to high salt concentrations and was observed to be linear with respect to polysaccharide concentration (Figure 2B).

Having shown uniform, efficient attachment of various polysaccharides to PLL-coated surfaces, we examined whether these surfaces could be exploited to detect glycosaminoglycan-protein interactions. A Microgrid II arrayer robot was used to deliver nanoliter volumes of heparin (unconjugated to fluorescein) in solutions ranging in concentration from 5 nM to 1000 nM, yielding spots that were ~100 μm in diameter. The microarray was incubated with FGF2, a member of a large family of growth factors involved in cell proliferation, development, and tumor angiogenesis and one of the best characterized HS-binding proteins [4, 37]. Binding of FGF2 was subsequently detected by incubation of the array with an anti-FGF2 antibody followed by a secondary Cy3-labeled antibody. We found that FGF2 bound to heparin on the array in a concentration-dependent manner (Figures 3A and 3B). Binding of FGF2 to as little as 0.01–10 fmol heparin could be detected on the microarray, indicating very high detection sensitivity. Interestingly, the S-shaped kinetic curve implied a complex binding mechanism consistent with cooperative binding of FGF2 to the polysaccharide. Analysis of the Hill plot gave a Hill coefficient of 6.1, suggestive of positive cooperativity. These results are similar to those of previous studies suggesting a multisite binding model for HS-protein interactions and/or the possibility of cooperative binding sites [6, 38–40]. Nonlinear regression analysis of the relative fluorescence intensity as a function of carbohydrate concentration afforded an EC_{50} value of

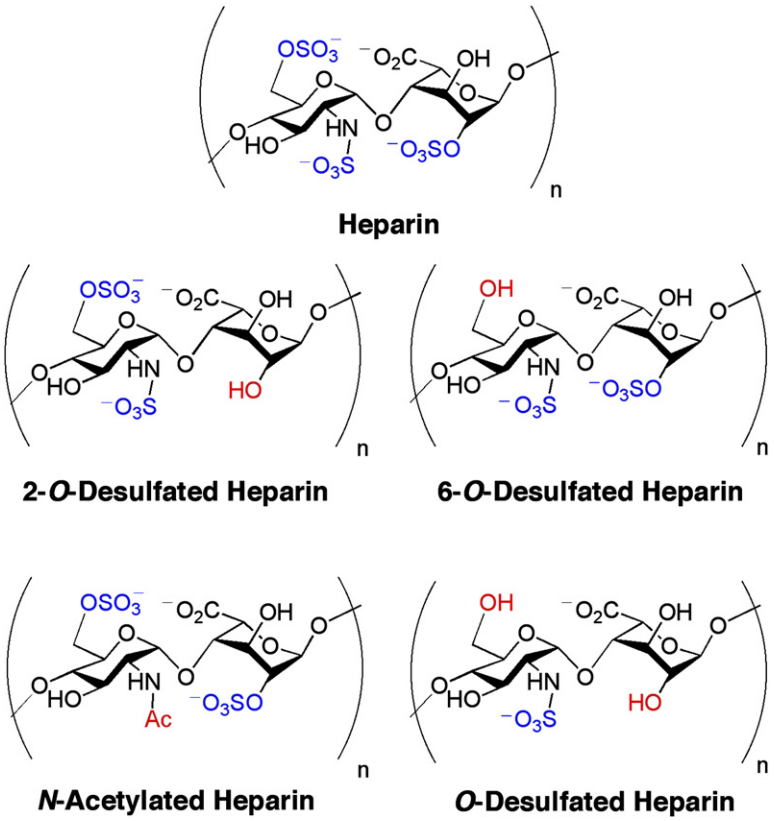

Figure 1. Heparin Polysaccharides Used for the Analysis of HS-Protein Interactions

For simplicity, the uronic acid residues are depicted as iduronic acid. n = ~20–22.

80.2 ± 2.7 nM, similar to K_d values determined for the binding of FGF2 to both heparin polysaccharides and oligosaccharides by surface plasmon resonance and optical biosensor binding assays [15, 41].

To determine whether the approach could be exploited to rapidly probe the sulfation specificities of proteins, we constructed a high-density microarray containing differentially sulfated HS derivatives. Specifically, heparin, 2-*O*-desulfated heparin, 6-*O*-desulfated heparin, fully *N*-acetylated heparin, and fully *O*-desulfated heparin were printed on a 1 cm × 1 cm grid (480 spots) at concentrations ranging from 5 nM to 100 μM. We found that FGF2 displayed distinct binding preferences for each sulfated form. Shown in Figure 3C is the relative binding of FGF2 to the HS variants at three different carbohydrate concentrations. By printing the polysaccharides over a wide concentration range, those concentrations that lie in a nearly linear part of the binding curve can be established, which enables comparison of the relative binding affinities of a protein to each sulfated variant. Strong binding of FGF2 to heparin and 6-*O*-desulfated heparin was observed, whereas the interaction was significantly reduced upon 2-*O*-desulfation, *N*-desulfation and acetylation, or complete *O*-desulfation of heparin. These findings agree with other biochemical studies, in which 2-*O*-sulfation, but not 6-*O*-sulfation, was shown to be crucial for the heparin-FGF2 interaction. Moreover, the results are reinforced by X-ray crystallographic studies demonstrating that the 2-*O*-sulfate and *N*-sulfate groups of heparin engage in electrostatic interactions with basic residues of FGF2 [42–44].

Quantitative analysis of the relative fluorescence intensities as a function of carbohydrate concentration afforded an EC_{50} value for 6-*O*-desulfated heparin of 83.3 ± 1.3 nM, comparable to that of heparin (Figure 3D). In contrast, removal of the 2-*O*-sulfate and *N*-sulfate groups significantly reduced the affinity of FGF2 for heparin (EC_{50} = 685.7 ± 17.0 and 666.4 ± 10.1 nM, respectively). As expected, no appreciable binding of FGF2 to completely *O*-desulfated heparin was observed. Although we obtained excellent quantitative data for FGF2, we note that some proteins are more amenable to this analysis than others. Importantly, all proteins that we examined showed linear binding to glycosaminoglycans within a given concentration range, which enabled direct comparison of the relative binding affinity of proteins for the different HS variants. Together, these results highlight the power of microarrays to enable rapid, systematic explorations into the importance of sulfation.

Sulfation Specificities Across the Fibroblast Growth Factor Family

The ability to analyze many glycosaminoglycan-protein interactions simultaneously facilitates comparisons across large protein families. Previous studies have suggested that different FGF members recognize distinct HS sulfation sequences, raising the interesting possibility that the sulfation patterns presented on the cell surface may help

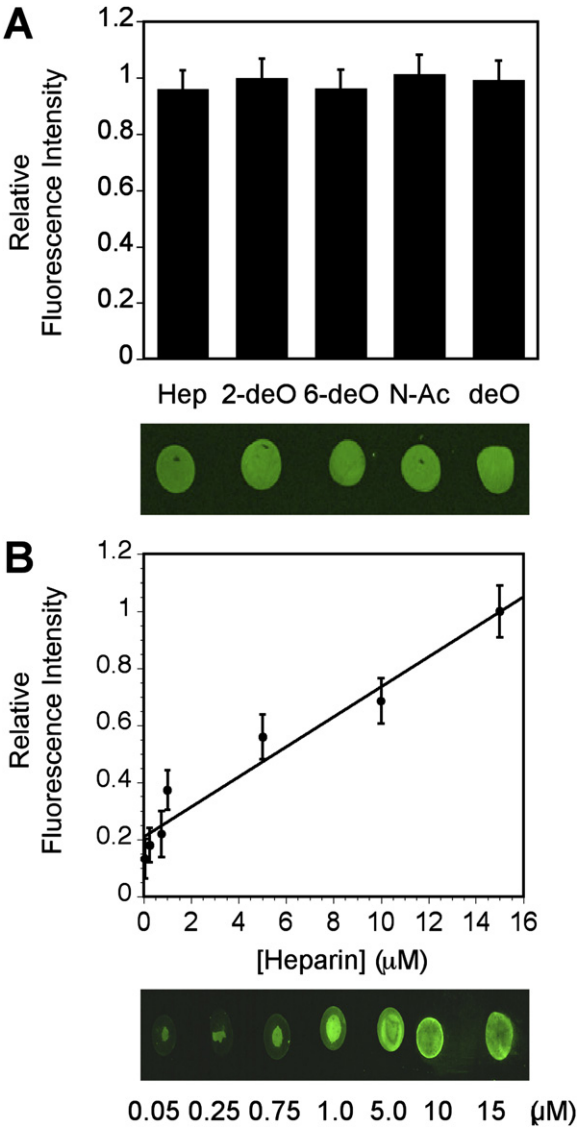

Figure 2. Heparin Polysaccharides Adhere Uniformly and Efficiently to Poly-L-Lysine-Coated Slides Independent of Sulfation Pattern

(A) Fluorescein-labeled heparin derivatives of varying sulfation patterns (1 pmol) were manually spotted onto PLL-coated slides. The fluorescence intensity was measured relative to an unconjugated fluorescein control.

(B) Fluorescein-conjugated heparin binds to PLL-coated slides in a linear, concentration-dependent manner.

Error bars represent the standard error of the mean (SEM) from four experiments.

to activate particular FGF-signaling pathways [43, 45, 46]. We examined the sulfation specificities of various members of the family, including FGF1, FGF4, FGF16, and FGF17. Notably, each family member exhibited a distinct sulfation preference (Figure 4). In contrast to FGF2, FGF1 showed a strong reduction in binding to 6-*O*-desulfated heparin relative to heparin and a more modest reduction in binding to 2-*O*-desulfated heparin. On the other hand, 2-*O*-desulfation and 6-*O*-desulfation led to a comparable reduction in FGF4 binding to heparin, suggesting that sulfation at both positions is equally important. In all cases, *N*-sulfation was found to be a critical determinant for binding. Our results are supported by previous studies indicating that FGF1 requires 6-*O*-sulfation and *N*-sulfation, but not 2-*O*-sulfation, for heparin binding [7, 47], whereas FGF4 requires sulfation of both the 2-*O*- and 6-*O*-positions [45].

We also characterized two new members of the FGF family, FGF16 and FGF17, whose sulfation specificities, to our knowledge, were unknown. FGF16 plays a role in the development of the heart [48], whereas FGF17 participates in the induction and patterning of the developing brain [49]. We found that FGF16 required sulfation at the 2-*O*-, 6-*O*-, and *N*-positions at low polysaccharide concentrations. Interestingly, at higher concentrations, binding of FGF16 to 6-*O*-desulfated heparin was observed, suggesting a greater importance for the 2-*O*-sulfate-position. With FGF17, we identified 6-*O*-sulfation and *N*-sulfation as key determinants for heparin binding. While 2-*O*-desulfation of heparin diminished the interaction, the loss of binding was less than that observed upon 6-*O*-desulfation, suggesting a greater role for 6-*O*-sulfation.

These findings demonstrate that the FGF family members exhibit distinct preferences for HS sulfation motifs, and they highlight the ease with which the sulfation specificities of HS-binding proteins can be elucidated by using microarrays. The enhanced affinity of FGF family members for particular sulfation motifs may be important during development, as the sulfotransferases involved in HS biosynthesis are differentially expressed in certain tissues and developmental stages [50, 51]. For instance, studies have shown that alternations in the HS sulfation pattern that favor FGF1 binding relative to FGF2, as well as changes in growth factor production from FGF2 to FGF1, occur as neural precursor cells cease to proliferate and begin to differentiate [50, 52, 53]. It will be interesting to examine whether the sulfation motifs uncovered by our microarrays for FGF16 and FGF17 are upregulated during organogenesis or brain development and modulate the activity of these important growth factors.

Sulfation Specificities of Axon Guidance Proteins

Glycosaminoglycan microarrays can also be exploited to study proteins that lack homology, but share a common function, in order to probe the involvement of HS in specific biological processes. For instance, previous studies have shown that HS interacts with slit2, a protein that directs axons toward specific targets in the developing brain [16, 54, 55]. However, the importance of sulfation in directing this interaction has not been examined. We also sought to investigate whether HS might interact with a variety of chemotactic proteins and thus participate more broadly in axon guidance.

We found that slit2 bound to heparin on the microarray, consistent with cellular studies in which ^{125}I-labeled slit interacted with the surface of HS-expressing cells and recent SPR studies with HS oligosaccharides (Figure 5A)

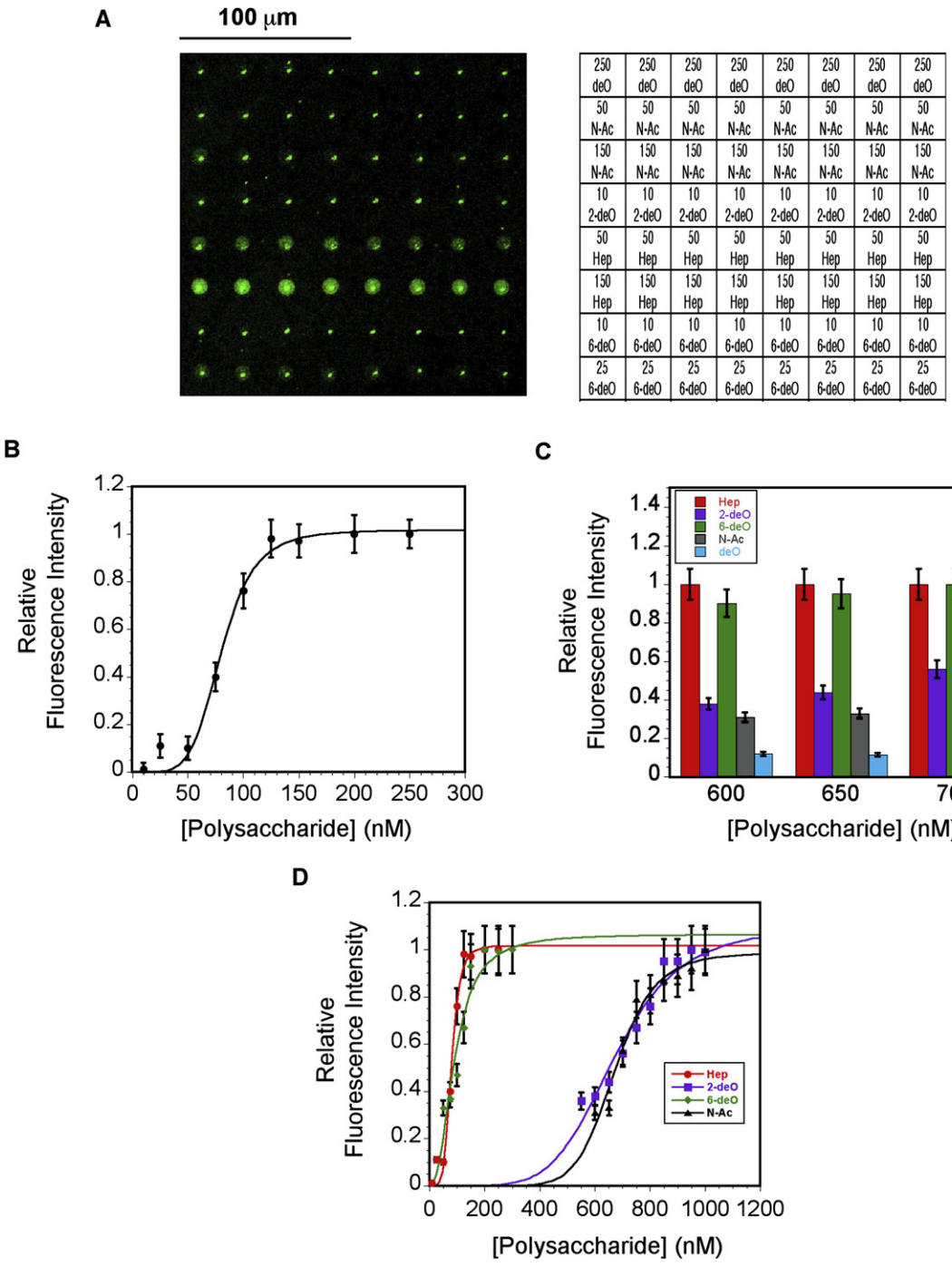

Figure 3. FGF2 Interacts with Heparin Polysaccharides on the Microarray and Favors Binding to Heparin and 6-*O*-Desulfated Heparin

(A) Representative image of a portion of the microarray. Multiple concentrations of heparin and heparin derivatives were spotted onto the microarray to create a pattern of 480 spots. The panel on the right indicates the corresponding polysaccharides and their concentrations (given in nM).

(B) Nonlinear regression analysis of the relative fluorescence intensity as a function of heparin concentration.

(C) Relative binding of FGF2 to various sulfated forms of heparin. The relative fluorescence intensities were normalized with respect to the highest observed fluorescence intensity on the array and were plotted at polysaccharide concentrations of 600, 650, and 700 nM, which lie in the linear part of the binding curve for 2-*O*-desulfated and *N*-acetylated heparin.

(D) Nonlinear regression analysis for the different sulfated variants. The relative fluorescence intensities were normalized with respect to the highest fluorescence intensity for each variant.

Error bars represent the SEM from four experiments.

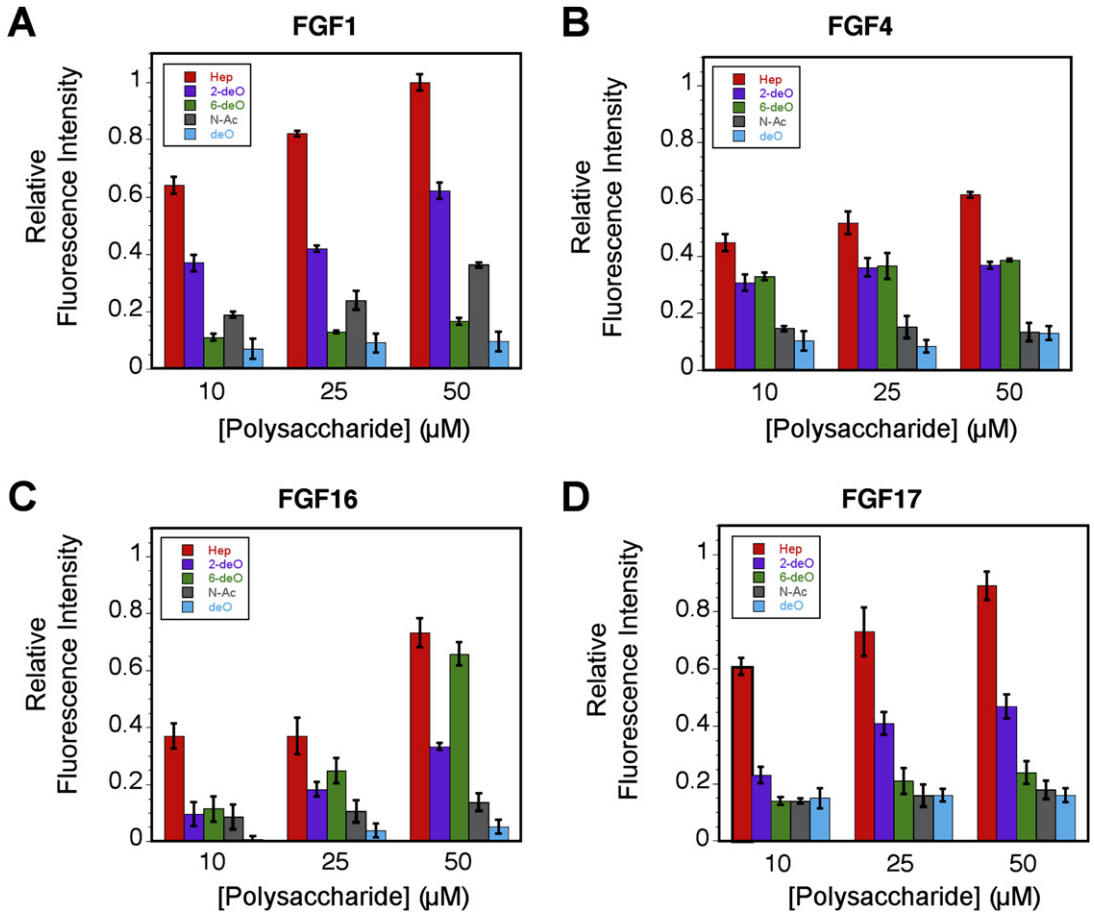

Figure 4. Comparison of the Sulfation Specificities of FGF Family Members

(A–D) Binding of (A) FGF1, (B) FGF4, (C) FGF16, and (D) FGF17 to the microarrays. The relative fluorescence intensities were plotted at polysaccharide concentrations of 10, 25, and 50 μM, which lie in the linear part of their binding curves. Error bars represent the SEM from four experiments.

[16, 54]. More importantly, we observed a strong preference of slit2 for 6-*O*-sulfated heparin, as indicated by a significant decrease in slit2 binding upon desulfation at the 6-position. By comparison, 2-*O*-desulfation elicited a weaker response. Slit2 also bound *N*-acetylated heparin poorly, indicating an important role for *N*-sulfation in binding. These results establish that slit2 has a preference for HS sulfation sequences that contain 6-*O*-sulfation and *N*-sulfation.

As independent confirmation of the microarray data, we examined the effects of HS sulfation on slit-mediated axon guidance. Olfactory bulb explants isolated from embryonic day 14.5 embryos were cocultured with slit2-expressing HEK293 cell aggregates in a collagen-Matrigel matrix. To visualize the axons, the cultures were stained with an anti-tau antibody and were examined by confocal fluorescence microscopy. As shown in Figure 6A, the secreted slit2 protein repels growing axons from the olfactory bulb. Previous studies have established that slit2 requires HS to mediate axon repulsion, as treatment of the cultures with heparinase or exogeneous HS abolished the repulsive activity of slit2 [54]. We therefore investigated the effects of the sulfated HS variants employed in our microarrays. The number of fasciculated axon bundles in the proximal and distal quadrants of the coculture was measured for each sulfated variant (Figure 6A). As expected, slit2 induced axonal repulsion, as indicated by the low proximal to distal ratio observed. We found that heparin and 2-*O*-desulfated heparin abolished the repulsive effects of slit2. In contrast, 6-*O*-desulfated and *N*-acetylated heparin had only modest effects on slit2-induced axonal repulsion, and completely *O*-desulfated heparin had no effect. These findings are consistent with the results obtained from our microarray analyses, which indicate that only heparin and 2-*O*-desulfated heparin interact strongly with slit2.

We next examined whether HS sulfation patterns are important for neuronal cell migration mediated by slit2. HEK293 cell aggregates expressing slit2 were cocultured with anterior subventricular zone (SVZa) explants from postnatal day 4–7 rats in a collagen-Matrigel matrix. Migrating neurons were visualized by transmitted light microscopy by using an inverted Zeiss microscope at 5× magnification. As shown in Figure 6B, slit2 repelled

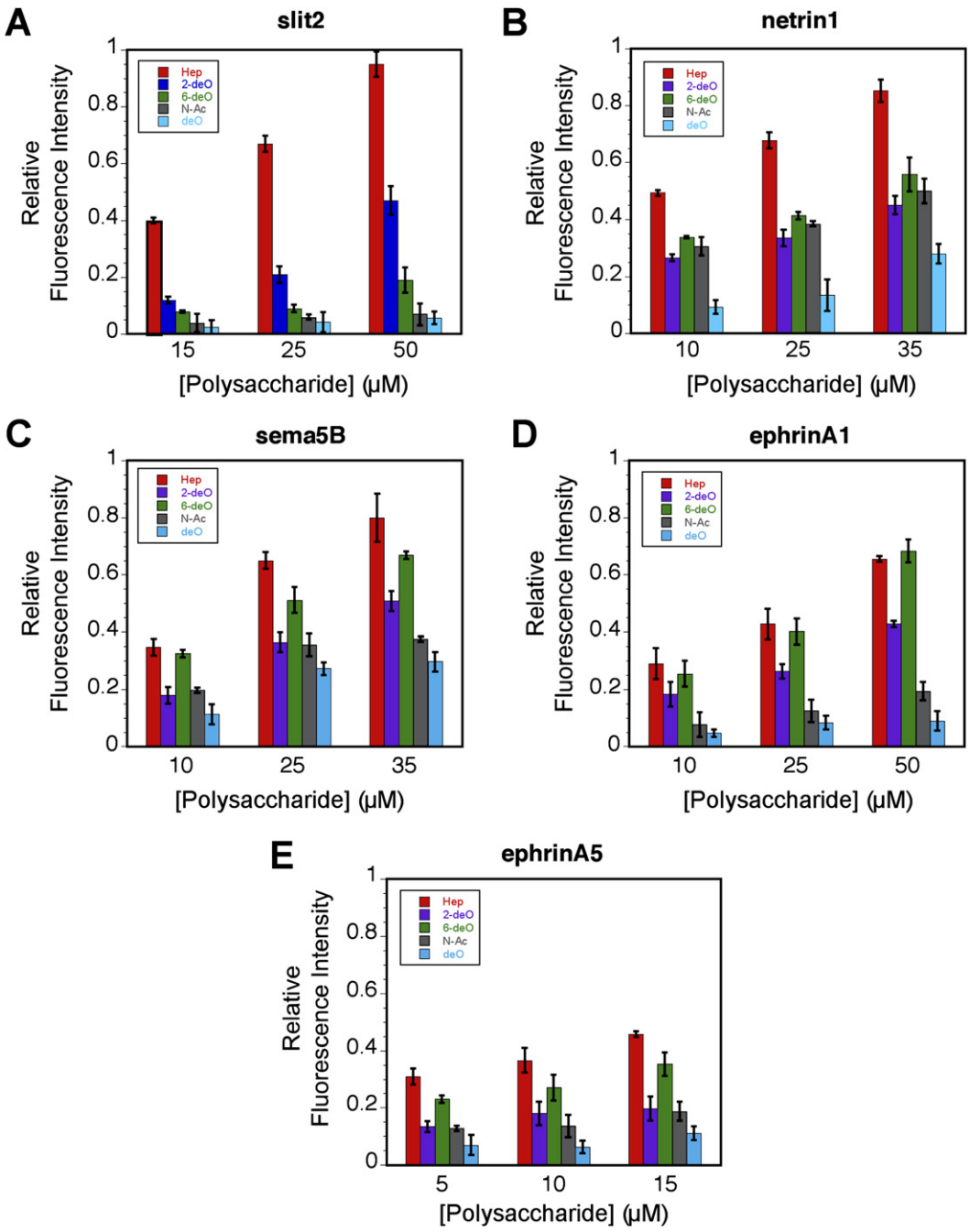

Figure 5. A Variety of Chemotactic Proteins Bind to Heparin/HS in a Sulfation-Dependent Manner

(A–E) Binding of (A) slit2, (B) netrin1, (C) sema5B, (D) ephrinA1, and (E) ephrinA5 to the microarrays. The relative fluorescence intensities were plotted at polysaccharide concentrations that lie in the linear part of their respective binding curves. Error bars represent the SEM from four experiments.

the migration of cells from the explants. Notably, the addition of heparin or 2-*O*-desulfated heparin to the medium abolished the repulsive activity of slit2 on neuronal migration. To quantify these effects, the ratio of the number of migrating neurons in the proximal versus the distal quadrants of the coculture was plotted (Figure 6B). The repulsion induced by slit2 can be seen by the presence of more neurons on the distal than the proximal side of the explant. In contrast, the addition of heparin or 2-*O*-desulfated heparin caused a more symmetrical, radial pattern of cells, in which equal numbers of neurons were found on both sides. Consistent with our microarray data, 6-*O*-desulfated heparin had only a slight effect on neuronal repulsion, and neither *N*-acetylated heparin nor completely de-*O*-sulfated heparin had an effect relative to the control (Figure 6B and data not shown). Together,

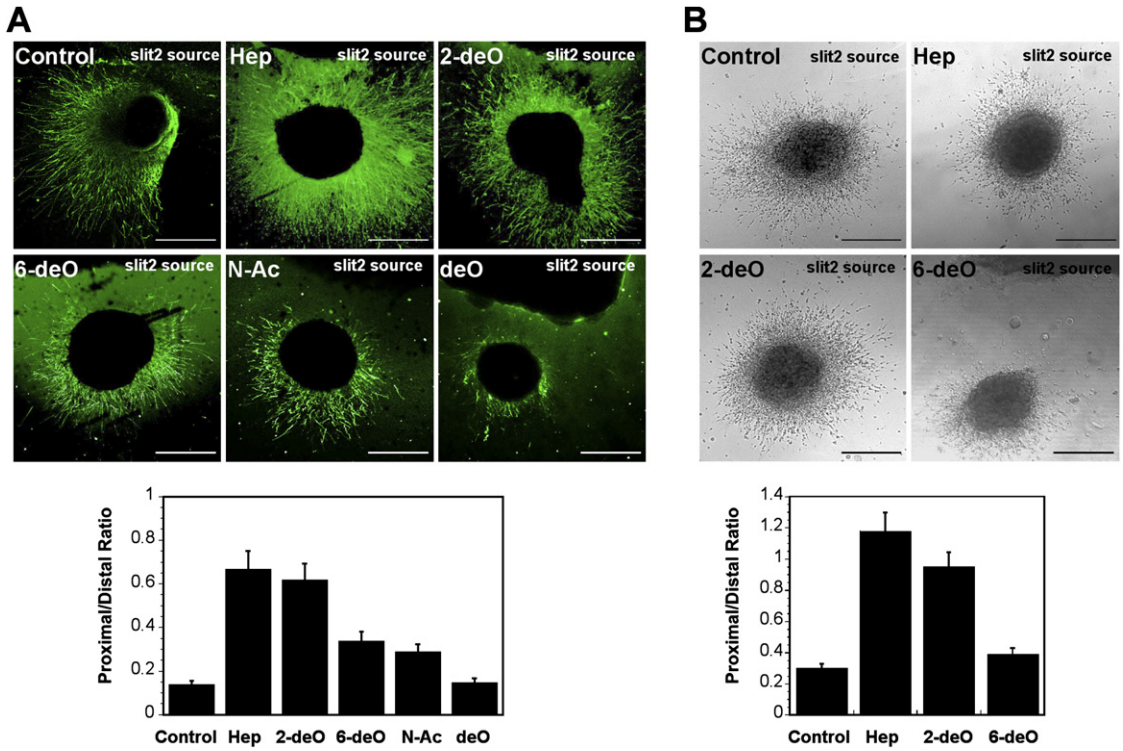

Figure 6. Slit2-Mediated Axon Guidance and Neuronal Migration Are Modulated by Specific HS Sulfation Patterns

(A) HEK293 cells expressing secreted slit2 were cocultured with embryonic day 14.5 rat olfactory bulbs in a 2:2:1 collagen:Matrigel:DMEM matrix in the presence of the indicated polysaccharides (30 μM). The cultures were immunostained with an anti-tau antibody and imaged by using confocal fluorescence microscopy. The number of fasciculated axon bundles in the proximal and distal quadrants of the coculture was measured for each polysaccharide variant. Error bars represent the SEM from three experiments. The scale bars indicate 500 μm.

(B) HEK293 cells expressing secreted slit2 were cocultured with postnatal day 3–6 rat SVZa explants in a 2:2:1 collagen:Matrigel:DMEM matrix in the presence of the indicated polysaccharides (30 μM). The migration of cells from the explant was visualized with confocal bright-field microscopy. *N*-acetylated and fully *O*-desulfated heparin had no effect on slit-mediated axon repulsion. The ratio of migrating neurons in the proximal versus distal quadrants was quantified relative to the explant. Error bars represent the SEM from three experiments. The scale bars indicate 500 μm.

these functional studies corroborate our microarray analyses and demonstrate that glycosaminoglycan microarrays can be used to gain new insights into the biological activities of HS-binding proteins.

To examine whether HS participates more broadly in axon guidance processes, we probed a panel of chemoattractant/chemorepellent proteins, including netrin1, ephrinA1, ephrinA5, and semaphorin5B (sema5B). Netrin functions as a chemoattractant on commissural axons when binding to its receptor DCC (deleted in colorectal cancer), whereas the ephrin family of proteins has been shown to regulate axon guidance through contact-mediated repulsion, inducing collapse of neuronal growth cones during development [55, 56]. The semaphorins are a large family of conserved secreted proteins that mediate chemotactic guidance events such as collapse of motor neuron growth cones and repulsion of growing axons [57]. Interestingly, semaphorin5A (sema5A) has been shown to interact with both HS and CS glycosaminoglycans [58]. Using the microarrays, we found that loss of 2-*O*-sulfation, 6-*O*-sulfation, or *N*-sulfation reduced the binding of netrin1 to heparin by approximately the same extent (Figure 5B). Complete *O*-desulfation nearly abolished netrin1 binding, particularly at lower concentrations of polysaccharide. These data suggest that netrin1 requires sulfation at the 2-*O*-, 6-*O*-, and *N*-positions, although we cannot exclude the possibility that netrin does not require a specific sulfation sequence for heparin binding. Either way, these findings are interesting, as the chemorepellent and chemoattractant proteins, slit and netrin, respectively, clearly interact with HS in a distinct manner. Remarkably, HS appears to be essential for the axon guidance activities of both netrin and slit. We found that netrin-mediated attraction was greatly diminished heparinase treatment or the addition of exogenous heparin to netrin1-olfactory bulb cocultures (see Figure S1 in the Supplemental Data available with this article online).

Sema5B exhibited a preference for specific sulfation motifs, as 2-*O*-desulfation and *N*-desulfation/acetylation of heparin reduced binding of sema5B by ~50%, whereas 6-*O*-desulfation had a lesser effect (Figure 5C). Moreover, to our knowledge, we demonstrate for the first time that ephrinA1 and ephrinA5 interact with HS and have a preference for both 2-*O*- and *N*-sulfation (Figures 5D and 5E). Thus, their binding profile more closely resembles that of sema5B and contrasts with that of slit2. EphrinA1 and

ephrinA5 share 68% homology, which likely accounts for their similar sulfation specificity. The ability of the ephrins to elicit a variety of biological responses is believed to arise from their promiscuous binding pattern (all ephrin A1–A5 ligands bind to all A1–A10 ephrin receptors) and the formation of higher-order ligand-receptor complexes [56, 59]. One possibility is that the specificity and multivalency of the ephrin/ephrin receptor interaction may be modulated by interactions with HS. Although this hypothesis remains to be tested, an intriguing observation is that ephrin null mutants in *C. elegans* enhance the phenotype of sulfotransferase null mutants, which suggests a possible functional connection between ephrin and HS sulfation [60].

It has become increasingly evident that HS plays an important role in axon targeting in the developing nervous system. For instance, mice lacking the HS-modifying enzyme *N*-acetylglucosamine *N*-deacetylase/*N*-sulfotransferase (Ndst1) exhibit severe developmental defects of the forebrain, including cerebral hypoplasia and lack of olfactory bulbs [61]. Studies of the *Xenopus* optic pathway indicate that inhibiting 2-*O*- and 6-*O*-sulfation causes developing axons to bypass their target, the tectum [62]. Furthermore, neuronal guidance defects such as incorrect midline patterning were observed in genetic studies of *C. elegans* mutants lacking certain sulfotransferases [63]. These studies suggest that the sulfation patterns of HS are critical for correct axon targeting. Our discovery of the unique affinities of axon guidance proteins for disparate HS sulfation patterns substantiates these previous studies. An intriguing possibility is that HS may participate in controlling the localization and activity of chemotactic proteins during neuronal development, possibly assisting in the creation of local protein gradients and facilitating interactions with cell surface receptors.

The variety of sulfation specificities observed by these proteins, coupled with other studies linking particular sulfotransferases to axon targeting [60–63], underscores the importance of elucidating the sulfation specificities of axon guidance proteins. Given the large number of potential sulfation sequences, the creation of focused libraries of synthetic oligosaccharides with defined sulfation motifs will be important in future studies. The microarrays described herein should help in this regard by allowing glycosaminoglycan-protein interactions to be probed rapidly and by providing valuable information to guide oligosaccharide library designs.

Comparisons Across Glycosaminoglycan Classes

In addition to versatility with respect to proteins, our microarray platform is compatible with all glycosaminoglycan subtypes, which permits systematic comparisons of protein binding across various classes. Such comparisons are important for understanding the specificities of glycosaminoglycan-binding proteins in vivo, where various subtypes may compete with one another for protein binding. We constructed microarrays containing heparin; HS; CS enriched in the CS-A, CS-C, CS-D, or CS-E sulfation motifs; dermatan sulfate (CS-B); KS; and hyaluronic acid (HA). The binding of FGF1 and FGF2 to the array was initially tested because previous studies have demonstrated that FGF1 interacts with HS, but not CS polysaccharides, whereas FGF2 recognizes both heparin and CS-E polysaccharides with similar binding affinity [64]. As expected, we found that FGF1 bound strongly to HS and heparin on the microarray and interacted only weakly with CS-E and other glycosaminoglycan classes (Figure 7). In contrast, FGF2 interacted with HS, heparin, and CS-E to a comparable extent. As further validation, we demonstrated that HA-binding protein (HABP) binds selectively to HA on the microarray.

The ability of various axon guidance proteins to interact with these glycosaminoglycan classes was next examined. Interestingly, all of the proteins recognized heparin, HS, and CS polysaccharides enriched in the CS-E motif (Figures 7D–7H). Little or no binding of the proteins to other glycosaminoglycans such as KS or HA was detected. In the case of ephrinA1, ephrinA5, and sema5B, weak binding to other CS polysaccharides and dermatan sulfate was observed, although the extent of binding was generally lower than that of heparin, HS, and CS-E. Notably, all of the proteins interacted weakly with polysaccharides enriched in the CS-D motif, despite the fact that CS-D and CS-E have the same number of sulfate groups per disaccharide unit. Thus, it appears that the precise placement of the sulfate groups, rather than nonspecific electrostatic effects, governs the binding of proteins to CS. Indeed, we have found previously that defined tetrasaccharides displaying two sequential CS-E sequences interact specifically with several proteins, including midkine, brain-derived neurotrophic factor (BDNF), and tumor necrosis factor-α (TNF-α) [22, 23]. Lastly, we validated our microarray results further by showing that CS-E polysaccharides abolish slit2-mediated repulsion of both axons and migrating neurons to the same extent as heparin (see Figures S2 and S3). Together, our studies suggest that CS-E and HS may modulate the activity of axon guidance proteins in vivo. In accordance with this hypothesis, it has recently been reported that sema5A attracts axons of the diencephalon in the presence of HS, but becomes repulsive toward the same axons when CS is present [58]. Interestingly, sema5B also appears to possess this dual ability to interact with both HS and CS glycosaminoglycans. Future studies will address the intriguing functional interplay between CS-E and HS.

SIGNIFICANCE

Despite growing recognition of the importance of glycosaminoglycans in many physiological processes, a detailed understanding of their structure-activity relationships has been lacking. Here, we report a facile, microarray-based platform that enables rapid interrogation of glycosaminoglycan-protein interactions without requiring specialized expertise in carbohydrate or surface chemistry. The key structural determinants responsible for protein binding, such as sulfate groups that participate in the interaction, are

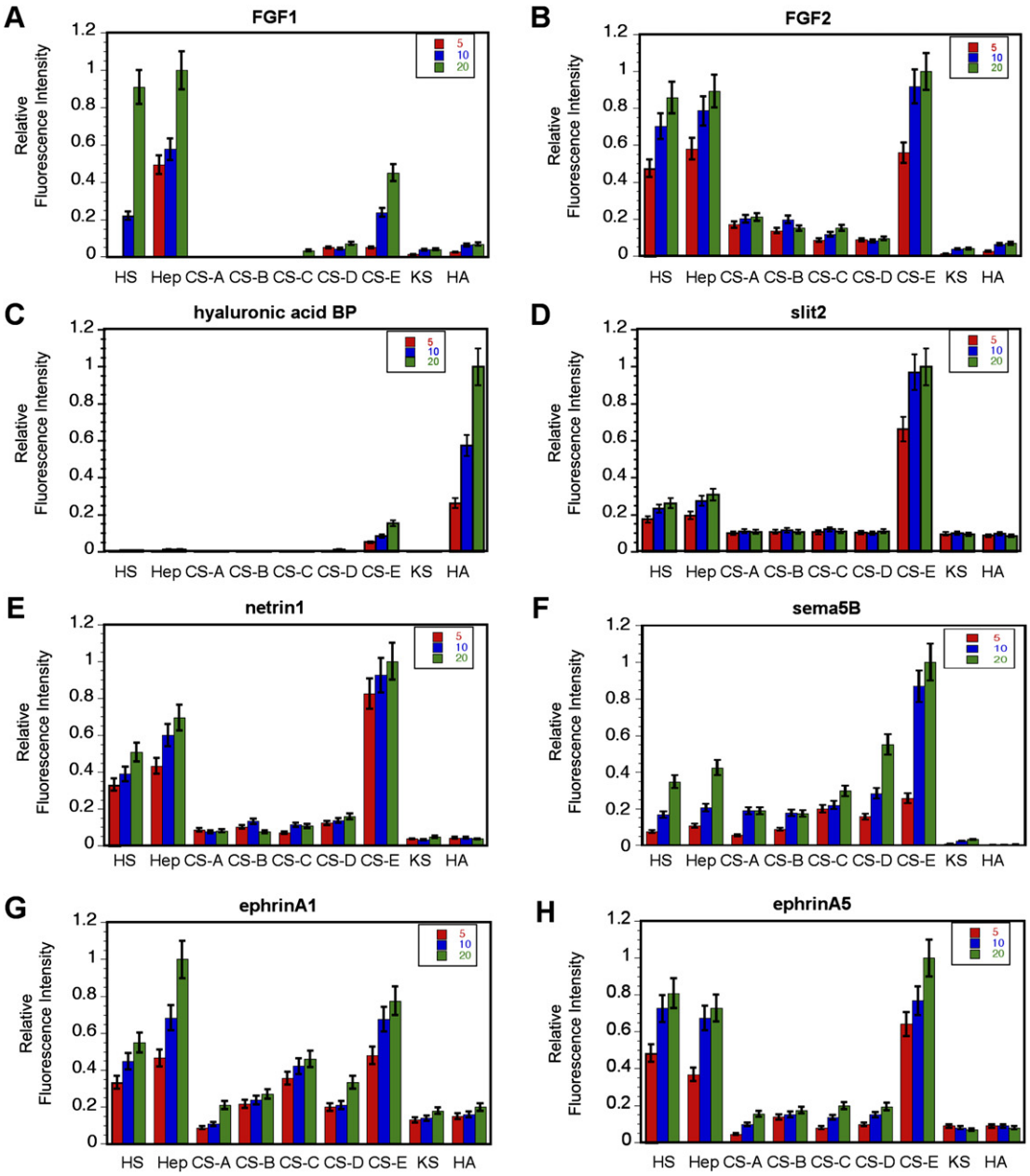

Figure 7. Comparisons among Glycosaminoglycan Classes

(A–H) Binding of (A) FGF1, (B) FGF2, (C) hyaluronic acid-binding protein, (D) slit2, (E) netrin1, (F) sema5B, (G) ephrinA1, and (H) ephrinA5 to heparan sulfate (HS), heparin (Hep), chondroitin sulfate-A (CS-A), dermatan sulfate (CS-B), chondroitin sulfate-C (CS-C), chondroitin sulfate-D (CS-D), chondroitin sulfate-E (CS-E), keratan sulfate (KS), and hyaluronic acid (HA). The microarrays were constructed from polysaccharide solutions that ranged in concentration from 5 nM to 25 μM. The relative fluorescence intensities were plotted at polysaccharide concentrations of 5, 10, and 20 μM, which lie in the linear region of the binding curves. Error bars represent the SEM from four experiments.

elucidated. Specificities can be compared across protein families or functional classes, and direct comparisons of HS, CS, and other glycosaminoglycans are possible, providing a more comprehensive understanding of protein specificity. We anticipate that the technology will enable profiling of protein-binding patterns to glycosaminoglycans isolated from different cell types, organs, or cell states. To illustrate the approach, we demonstrated that FGF family members recognize distinct sulfation motifs. Moreover, we discovered several HS-binding proteins, including FGF17, ephrinA5, and ephrinA6. We also found that HS binds to several classes of chemotactic proteins, and we show that HS is required for netrin-mediated axonal attraction. Furthermore, we compared the interactions of these proteins with various glycosaminoglycan classes

and found that many proteins that recognize HS also recognize CS-E. This suggests that numerous HS-binding proteins may be subject to regulation by both HS and CS glycosaminoglycans.

An important goal for the future will be to understand the sulfation specificities in greater detail. Given the large number of potential sequences, the creation of focused libraries of synthetic oligosaccharides containing a limited set of sulfation motifs will be essential. The microarrays described here will help define the specificities of proteins and guide synthetic library designs. The ability to discover new glycosaminoglycan-binding proteins and elucidate their specificities promises to accelerate the identification of glycosaminoglycan-binding proteins and provide a broader understanding of their physiological roles.

EXPERIMENTAL PROCEDURES

Materials

Heparin polysaccharides were purchased from Neoparin (Alameda, CA). The uronic acid composition of heparin and its sulfated derivatives was ~75% L-iduronic acid and 25% D-glucuronic acid, as stated by the manufacturer. CS-A, CS-C, CS-D, CS-E, and KS polysaccharides were purchased from Seikagaku America (Fallmouth, MA). CS-B and HA were purchased from Sigma-Aldrich (St. Louis, MO). Human FGF1, FGF2, FGF4, FGF16, FGF17, ephrinA5, mouse ephrinA1, chicken netrin1, and their respective antibodies were purchased from R&D Systems (Minneapolis, MN). Hyaluronic acid-binding protein and its corresponding antibody were purchased from U.S. Biologicals (Swampscott, MA). (5-(((2-(carbohydrazino)methyl)-thio)acetyl)aminofluorescein was purchased from Invitrogen (Carlsbad, CA). Myc-tagged human slit2- and HA-tagged chicken netrin1-expressing HEK293 cells were a gift from Professor Yi Rao (Northwestern University; Chicago, IL) [65, 66]. HEK293 cells expressing c-myc-tagged human slit2 were grown in 100 mm dishes for 3 days and were extracted with 5 ml of 1 M NaCl in the presence of a cocktail of protease inhibitors (Roche Diagnostics; Indianapolis, IN) as previously reported [54]. The extract was then concentrated, and the buffer was exchanged for PBS (137 mM NaCl, 10 mM Na_2HPO_4, 2.7 mM KCl [pH 7.4]) by using Centricon filters (30,000 MWCO; Millipore; Billerica, MA). Fc-tagged human AP-Sema5B[TSR1-4]-Fc was a generous gift from Professor Alex Kolodkin (Johns Hopkins University; Baltimore, MD). The AP-Sema5B[TSR1-4] construct was transfected into HEK293 cells and was grown in 100 mm dishes for 2–4 days. The culture media (100 ml) containing ~5 nM of the secreted sema5B protein was collected, centrifuged for 30 min at 15,000 × g, concentrated to 1–2 μM with Centricon filters (10,000 MWCO), and dialyzed into PBS. The PLL-coated glass slides were purchased from Erie Scientific (Portsmouth, NH). Timed-pregnant Sprague Dawley rats were purchased from Charles River Laboratories (Wilmington, MA). All handling and experimental procedures with animals were approved by the Institutional Animal Care and Use Committee at Caltech and were performed in accordance with the Public Health Service Policy on Humane Care and Use of Laboratory Animals.

Heparin-Fluorophore Labeling and Surface Adherence Studies

Five molar excess of 5-(((2-(carbohydrazino)methyl)-thio)acetyl)aminofluorescein was incubated with heparin, 2-*O*-desulfated heparin, 6-*O*-desulfated heparin, fully *O*-desulfated heparin, *N*-desulfated/*N*-acetylated heparin in 0.2 M borate buffer (pH 8.0) and 100 mM NaCl at 37°C for 48 hr. The conjugated heparin derivatives were then dialyzed in H_2O to remove any unreacted fluorophore. For the fluorescein control molecule, 2 μmol 5-(((2-(carbohydrazino)methyl)-thio)acetyl)aminofluorescein was reacted with acetaldehyde (1.5 equivalents) in DMF:H_2O (1:1; 200 μl) at room temperature for 24 hr and was subsequently purified by using a 1 ml C18 Sep-Pak column. Fractions (1 ml) were collected by using an increasing gradient of acetonitrile in water (0%–90%). The product eluted at ~85% acetonitrile. The fraction containing the product was confirmed by mass spectrometry. The concentrations of the compounds were adjusted to 1 μM by using the extinction coefficient of the fluorophore (ε = 70,000 $M^{-1}cm^{-1}$) at 518 nm. The compounds (1 μl) were then manually spotted onto PLL-coated slides in quadruplicate and were dried in a 70% humidity chamber overnight. The resulting microarrays were analyzed for fluorescence signal intensity and spot morphology by using a GenePix 5000a scanner and were placed in a dust-free chamber overnight. The slides were then washed with 0.5 M aqueous NaCl for 30 min with gentle rocking, followed by PBS (5 × 10 min), dried under a gentle stream of N_2. Signal intensities were then recorded. Comparison of signal intensities before and after washing yielded the same extent of adherence of the polysaccharides to the microarray, ~86% based on the extinction coefficient of the fluorophore.

Generation of Microarrays

The relative concentrations of heparin, HS, CS, and KS polysaccharides were calibrated to one another by using the carbazole assay for uronic acid residues [67]. Briefly, the acid borate reagent (1.5 ml of a solution of 0.80 g sodium tetraborate in 16.6 ml H_2O and 83.3 ml sulfuric acid) was added to 20 ml glass vials with teflon caps. The polysaccharides (50 μl of a 4 mg/ml stock in H_2O) were added, and the solutions were placed in a boiling water bath for 10 min. After cooling and the addition of the carbazole reagent (50 μl of 0.1% w/v carbazole in 100% ethanol), the solutions were boiled for 15 min. The absorbance was measured at 530 nm and compared to a D-glucuronolactone standard in H_2O. Solutions of the polysaccharides (10 μl $well^{-1}$ in a 384-well plate) were spotted onto PLL-coated slides by using a Microgrid II arrayer (Biorobotics; Cambridge, UK) at room temperature and 50% humidity. Solution concentrations ranged from 5 nM to 100 μM, and the arrayer printed 1 nl of each concentration eight times. The resulting arrays were incubated in a 70% humidity chamber at room temperature overnight and then stored in a low-humidity, dust-free dessicator.

Protein-Binding Analyses

The slides were blocked with 3% bovine serum albumin (BSA) in PBS (5 ml) with gentle rocking at 37°C for 1 hr. These conditions were empirically determined to reduce nonspecific binding of proteins to the microarray and to provide optimal signal to noise ratios (an average of 10:1). A 2 cm box was drawn around the polysaccharide spots with a hydrophobic slide marker (Super Pap Pen, Research Products International Corp.; Mount Prospect, IL) prior to blocking. Human FGF1, FGF2, FGF4, FGF16, FGF17, ephrinA1, slit2, sema5B, hyaluronic acid-binding protein, mouse ephrinA5, or chicken netrin1 was reconstituted in 1% BSA in PBS, added to the slides in 50 μl quantities at a concentration of 1–2 μM, and incubated in a humidity chamber (empty pipette tip box containing 10 ml brine in the bottom) for 1 hr at room temperature. The slides were then washed five times for 3 min each in PBS (5 ml) while gently rocking. After the washes, the slides were incubated with 5 ml of the appropriate primary antibody in 1% BSA in PBS solution with gentle rocking for 1 hr. Optimal concentrations were determined for each antibody (1:500 for anti-FGF1; 1:1000 for anti-FGF2, anti-FGF4, anti-FGF16, anti-netrin1, and anti-myc [slit2]; 1:2000 for anti-FGF17). The slides were then washed five times for 3 min each in PBS (5 ml) while gently rocking. Next, the slides were incubated with 5 ml of a secondary IgG antibody conjugated to either Cy3 or Cy5 in the dark with gentle rocking for 1 hr (1:5000, Molecular Probes), washed with PBS followed by H_2O, and then dried under a gentle stream of N_2. A human IgG antibody conjugated to Cy3 was used for Fc-tagged ephrinA1, ephrinA5, and sema5B (1:5000, Molecular Probes). All incubations and washes were carried out at room temperature unless otherwise noted. The microarrays were analyzed at 532 nm for Cy3 or 635 nm for Cy5 by using a GenePix 5000a scanner, and fluorescence quantification was performed by

using GenePix 6.0 software with correction for local background. Mild signal anisotropy is a common occurrence at low concentrations in carbohydrate microarrays [25, 29]. To ensure accurate signal quantification, the average signal intensity was calculated over a fixed area for all spots. No fluorescence intensity was observed with controls performed with primary and secondary antibodies alone. Results were plotted with Kaleidagraph 6.0 software. Each protein was analyzed in triplicate, and the data represent an average of 5–8 spots for a given carbohydrate concentration.

Dissociation Constant Measurements

The EC_{50} values for binding of FGF2 to the various heparin/HS forms were calculated from nonlinear regression analysis of the relative fluorescence intensity as a function of carbohydrate concentration. Cooperative binding of FGF2 to HS polysaccharides on the microarray surface was observed, consistent with the Hill equation:

$$f = \frac{f_{max} \cdot [HS]^n}{EC_{50}^n + [HS]^n} + f_o, \quad (1)$$

where f is the observed fluorescence intensity, f_{max} is the fluorescence intensity at saturation, f_o is the initial fluorescence, [HS] is the carbohydrate concentration, and n is the Hill coefficient.

Cell and Tissue Culture

Stable HEK293 cell lines expressing human slit2 or chicken netrin1 were maintained in DMEM supplemented with 10% fetal bovine serum and antibiotics in a 5% CO_2-humidified incubator at 37°C. Cellular aggregates were prepared by the hanging drop method [68]. For the axon guidance assay, olfactory bulb explants were isolated with a tungsten needle from timed-pregnant rats at embryonic day 14.5 and were cocultured in a 2:2:1 Matrigel:collagen:DMEM mixture with HEK293 aggregates expressing either slit2 or netrin1. In the case of the neuronal migration assay, SVZa explants were isolated from the rostral migratory stream of postnatal day 4–7 rat olfactory bulbs and were cocultured with HEK293 aggregates expressing slit2 in a 2:2:1 Matrigel: collagen:DMEM mixture as previously described [69]. CS-E, heparin, 2-*O*-desulfated heparin, 6-*O*-desulfated heparin, *N*-acetylated heparin, or fully *O*-desulfated heparin (30 μM) was added to the Matrigel mixture and media in both the axon guidance and neuronal migration assays. The cocultures for both assays were incubated at 37°C for 48 hr. For the netrin1 axon guidance assay, either 30 μM heparin or 5 U/ml heparinase III (Sigma) was added to the cocultures. Quantification was performed by measuring the number of migrating neurons or fasciculated axon bundles in the proximal versus distal quadrants of the coculture as described previously [70]. All experiments were done in triplicate to ensure reproducibility.

Imaging and Immunostaining

The olfactory bulb cocultures were rinsed once with PBS, fixed in 4% paraformaldehyde for 20 min at room temperature, washed twice with PBS, permeabilized in 0.3% Triton X-100 for 5 min at room temperature, and washed twice with PBS. Nonspecific binding was blocked with 3% BSA for 1 hr at room temperature. The blocking solution was rinsed off once with PBS. The olfactory bulb cocultures were then incubated with an anti-tau antibody (rabbit polyclonal, 1:500; Sigma) in 3% BSA for 2 hr at room temperature. Excess antibody was washed away five times with PBS. Anti-rabbit IgG Alexa Fluor 488 (1:500; Invitrogen) was added for 1 hr at 37°C in 3% BSA. Excess secondary antibody was washed off five times with PBS. The cocultures were imaged with a Zeiss Axiovert 100M inverted confocal laser microscope in the Biological Imaging Center in the Beckman Institute at Caltech. The images were captured with LSM Pascal software by using 5×, 10×, or 20× objectives.

Supplemental Data

Supplemental Data include the effects of heparin and CS-E on netrin1-mediated chemoattraction and slit2-mediated chemorepulsion, respectively, and are available at http://www.chembiol.com/cgi/content/full/14/2/195/DC1/.

ACKNOWLEDGMENTS

We thank Dr. J.L. Riechmann, Director of the Millard and Muriel Jacobs Genetics and Genomics Laboratory at the California Institute of Technology, for assistance with printing the microarrays, and Dr. S.E. Tully, C.J. Rogers, and Dr. M.C. Bryan for helpful discussions. We also thank M. Ward, Professor Y. Rao, and Professor J. Wu for the slit2 and netrin1 cell lines and for training in neuronal migration and coculture techniques. We thank Professor A. Kolodkin and R. Matsuoka for the generous gift of sema5B. This research was supported by a National Science Foundation Minority Postdoctoral Fellowship (E.L.S.), the National Institutes of Health (RO1 NS045061), the American Cancer Society (RSG-05-106-01-CDD), and the Tobacco-Related Disease Research Program (14RT-0034).

Received: August 30, 2006
Revised: December 13, 2006
Accepted: December 28, 2006
Published: February 23, 2007

REFERENCES

1. Capila, I., and Linhardt, R.J. (2002). Heparin-protein interactions. Angew. Chem. Int. Ed. Engl. *41*, 391–412.
2. Whitelock, J.M., and Iozzo, R.V. (2005). Heparan sulfate: a complex polymer charged with biological activity. Chem. Rev. *105*, 2745–2764.
3. Petitou, M., and van Boeckel, C.A. (2004). A synthetic antithrombin III binding pentasaccharide is now a drug! What comes next? Angew. Chem. Int. Ed. Engl. *43*, 3118–3133.
4. Waksman, G., and Herr, A.B. (1998). New insights into heparin-induced FGF oligomerization. Nat. Struct. Biol. *5*, 527–530.
5. Pellegrini, L., Burke, D.F., von Delft, F., Mulloy, B., and Blundell, T.L. (2000). Crystal structure of fibroblast growth factor receptor ectodomain bound to ligand and heparin. Nature *407*, 1029–1034.
6. Powell, A.K., Yates, E.A., Fernig, D.G., and Turnbull, J.E. (2004). Interactions of heparin/heparan sulfate with proteins: appraisal of structural factors and experimental approaches. Glycobiology *14*, 17R–30R.
7. Jemth, P., Kreuger, J., Kusche-Gullberg, M., Sturiale, L., Gimenez-Gallego, G., and Lindahl, U. (2002). Biosynthetic oligosaccharide libraries for identification of protein-binding heparan sulfate motifs. Exploring the structural diversity by screening for fibroblast growth factor (FGF)1 and FGF2 binding. J. Biol. Chem. *277*, 30567–30573.
8. Ishihara, M., Tyrrell, D.J., Stauber, G.B., Brown, S., Cousens, L.S., and Stack, R.J. (1993). Preparation of affinity-fractionated, heparin-derived oligosaccharides and their effects on selected biological activities mediated by basic fibroblast growth factor. J. Biol. Chem. *268*, 4675–4683.
9. Wu, Z.L., Zhang, L., Yabe, T., Kuberan, B., Beeler, D.L., Love, A., and Rosenberg, R.D. (2003). The involvement of heparan sulfate (HS) in FGF1/HS/FGFR1 signaling complex. J. Biol. Chem. *278*, 17121–17129.
10. Feitsma, K., Hausser, H., Robenek, H., Kresse, H., and Vischer, P. (2000). Interaction of thrombospondin-1 and heparan sulfate from endothelial cells. Structural requirements of heparan sulfate. J. Biol. Chem. *275*, 9396–9402.
11. Pisano, C., Aulicino, C., Vesci, L., Casu, B., Naggi, A., Torri, G., Ribatti, D., Belleri, M., Rusnati, M., and Presta, M. (2005). Undersulfated, low-molecular-weight glycol-split heparin as an antiangiogenic VEGF antagonist. Glycobiology *15*, 1C–6C.
12. Foxall, C., Holme, K.R., Liang, W., and Wei, Z. (1995). An enzyme-linked immunosorbent assay using biotinylated heparan sulfate to

evaluate the interactions of heparin-like molecules and basic fibroblast growth factor. Anal. Biochem. *231*, 366–373.

13. Sweeney, M.D., Yu, Y., and Leary, J.A. (2006). Effects of sulfate position on heparin octasaccharide binding to CCL2 examined by tandem mass spectrometry. J. Am. Soc. Mass Spectrom. *17*, 1114–1119.
14. Keiser, N., Venkataraman, G., Shriver, Z., and Sasisekharan, R. (2001). Direct isolation and sequencing of specific protein-binding glycosaminoglycans. Nat. Med. *7*, 123–128.
15. Ibrahimi, O.A., Zhang, F., Hrstka, S.C., Mohammadi, M., and Linhardt, R.J. (2004). Kinetic model for FGF, FGFR, and proteoglycan signal transduction complex assembly. Biochemistry *43*, 4724–4730.
16. Zhang, F., Ronca, F., Linhardt, R.J., and Margolis, R.U. (2004). Structural determinants of heparan sulfate interactions with Slit proteins. Biochem. Biophys. Res. Commun. *317*, 352–357.
17. Thompson, L.D., Pantoliano, M.W., and Springer, B.A. (1994). Energetic characterization of the basic fibroblast growth factor-heparin interaction: identification of the heparin binding domain. Biochemistry *33*, 3831–3840.
18. Feizi, T., Fazio, F., Chai, W., and Wong, C.H. (2003). Carbohydrate microarrays - a new set of technologies at the frontiers of glycomics. Curr. Opin. Struct. Biol. *13*, 637–645.
19. Wang, D. (2003). Carbohydrate microarrays. Proteomics *3*, 2167–2175.
20. Huang, C.Y., Thayer, D.A., Chang, A.Y., Best, M.D., Hoffmann, J., Head, S., and Wong, C.H. (2006). Carbohydrate microarray for profiling the antibodies interacting with Globo H tumor antigen. Proc. Natl. Acad. Sci. USA *103*, 15–20.
21. Adams, E.W., Ratner, D.M., Bokesch, H.R., McMahon, J.B., O'Keefe, B.R., and Seeberger, P.H. (2004). Oligosaccharide and glycoprotein microarrays as tools in HIV glycobiology: glycan-dependent gp120/protein interactions. Chem. Biol. *11*, 875–881.
22. Gama, C.I., Tully, S.E., Sotogaku, N., Clark, P.M., Rawat, M., Vaidehi, N., Goddard, W.A., 3rd, Nishi, A., and Hsieh-Wilson, L.C. (2006). Sulfation patterns of glycosaminoglycans encode molecular recognition and activity. Nat. Chem. Biol. *2*, 467–473.
23. Tully, S.E., Rawat, M., and Hsieh-Wilson, L.C. (2006). Discovery of a TNF-α antagonist using chondroitin sulfate microarrays. J. Am. Chem. Soc. *128*, 7740–7741.
24. Blixt, O., Head, S., Mondala, T., Scanlan, C., Huflejt, M.E., Alvarez, R., Bryan, M.C., Fazio, F., Calarese, D., Stevens, J., et al. (2004). Printed covalent glycan array for ligand profiling of diverse glycan binding proteins. Proc. Natl. Acad. Sci. USA *101*, 17033–17038.
25. de Paz, J.L., Noti, C., and Seeberger, P.H. (2006). Microarrays of synthetic heparin oligosaccharides. J. Am. Chem. Soc. *128*, 2766–2767.
26. Park, S., Lee, M.R., Pyo, S.J., and Shin, I. (2004). Carbohydrate chips for studying high-throughput carbohydrate-protein interactions. J. Am. Chem. Soc. *126*, 10794.
27. Fukui, S., Feizi, T., Galustian, C., Lawson, A.M., and Chai, W. (2002). Oligosaccharide microarrays for high-throughput detection and specificity assignments of carbohydrate-protein interactions. Nat. Biotechnol. *20*, 1011–1017.
28. Houseman, B.T., and Mrksich, M. (2002). Carbohydrate arrays for the evaluation of protein binding and enzymatic modification. Chem. Biol. *9*, 443–454.
29. Zhi, Z.L., Powell, A.K., and Turnbull, J.E. (2006). Fabrication of carbohydrate microarrays on gold surfaces: direct attachment of nonderivatized oligosaccharides to hydrazide-modified self-assembled monolayers. Anal. Chem. *78*, 4786–4793.
30. Carion, O., Lefebvre, J., Dubreucq, G., Dahri-Correia, L., Correia, J., and Melnyk, O. (2006). Polysaccharide microarrays for polysaccharide-platelet-derived-growth-factor interaction studies. ChemBioChem *7*, 817–826.
31. Willats, W.G., Rasmussen, S.E., Kristensen, T., Mikkelsen, J.D., and Knox, J.P. (2002). Sugar-coated microarrays: a novel slide surface for the high-throughput analysis of glycans. Proteomics *2*, 1666–1671.
32. Pirrung, M.C. (2002). How to make a DNA chip. Angew. Chem. Int. Ed. Engl. *41*, 1277–1289.
33. Schena, M., Shalon, D., Davis, R.W., and Brown, P.O. (1995). Quantitative monitoring of gene expression patterns with a complementary DNA microarray. Science *270*, 467–470.
34. Maccarana, M., Casu, B., and Lindahl, U. (1993). Minimal sequence in heparin/heparan sulfate required for binding of basic fibroblast growth factor. J. Biol. Chem. *268*, 23898–23905.
35. Pankonin, M.S., Gallagher, J.T., and Loeb, J.A. (2005). Specific structural features of heparan sulfate proteoglycans potentiate neuregulin-1 signaling. J. Biol. Chem. *280*, 383–388.
36. Spillmann, D., Witt, D., and Lindahl, U. (1998). Defining the interleukin-8-binding domain of heparan sulfate. J. Biol. Chem. *273*, 15487–15493.
37. Ornitz, D.M., and Itoh, N. (2001). Fibroblast growth factors. Genome Biol. *2*, Reviews3005.
38. Lustig, F., Hoebeke, J., Ostergren-Lunden, G., Velge-Roussel, F., Bondjers, G., Olsson, U., Ruetschi, U., and Fager, G. (1996). Alternative splicing determines the binding of platelet-derived growth factor (PDGF-AA) to glycosaminoglycans. Biochemistry *35*, 12077–12085.
39. Vives, R.R., Sadir, R., Imberty, A., Rencurosi, A., and Lortat-Jacob, H. (2002). A kinetics and modeling study of RANTES(9–68) binding to heparin reveals a mechanism of cooperative oligomerization. Biochemistry *41*, 14779–14789.
40. Nugent, M.A., and Edelman, E.R. (1992). Kinetics of basic fibroblast growth factor binding to its receptor and heparan sulfate proteoglycan: a mechanism for cooperactivity. Biochemistry *31*, 8876–8883.
41. Delehedde, M., Lyon, M., Gallagher, J.T., Rudland, P.S., and Fernig, D.G. (2002). Fibroblast growth factor-2 binds to small heparin-derived oligosaccharides and stimulates a sustained phosphorylation of p42/44 mitogen-activated protein kinase and proliferation of rat mammary fibroblasts. Biochem. J. *366*, 235–244.
42. Faham, S., Hileman, R.E., Fromm, J.R., Linhardt, R.J., and Rees, D.C. (1996). Heparin structure and interactions with basic fibroblast growth factor. Science *271*, 1116–1120.
43. Faham, S., Linhardt, R.J., and Rees, D.C. (1998). Diversity does make a difference: fibroblast growth factor-heparin interactions. Curr. Opin. Struct. Biol. *8*, 578–586.
44. Schlessinger, J., Plotnikov, A.N., Ibrahimi, O.A., Eliseenkova, A.V., Yeh, B.K., Yayon, A., Linhardt, R.J., and Mohammadi, M. (2000). Crystal structure of a ternary FGF-FGFR-heparin complex reveals a dual role for heparin in FGFR binding and dimerization. Mol. Cell *6*, 743–750.
45. Ashikari-Hada, S., Habuchi, H., Kariya, Y., Itoh, N., Reddi, A.H., and Kimata, K. (2004). Characterization of growth factor-binding structures in heparin/heparan sulfate using an octasaccharide library. J. Biol. Chem. *279*, 12346–12354.
46. Kariya, Y., Kyogashima, M., Suzuki, K., Isomura, T., Sakamoto, T., Horie, K., Ishihara, M., Takano, R., Kamei, K., and Hara, S. (2000). Preparation of completely 6-O-desulfated heparin and its ability to enhance activity of basic fibroblast growth factor. J. Biol. Chem. *275*, 25949–25958.
47. Kreuger, J., Prydz, K., Pettersson, R.F., Lindahl, U., and Salmivirta, M. (1999). Characterization of fibroblast growth factor 1 binding heparan sulfate domain. Glycobiology *9*, 723–729.

48. Lavine, K.J., Yu, K., White, A.C., Zhang, X., Smith, C., Partanen, J., and Ornitz, D.M. (2005). Endocardial and epicardial derived FGF signals regulate myocardial proliferation and differentiation in vivo. Dev. Cell *8*, 85–95.

49. Hoshikawa, M., Ohbayashi, N., Yonamine, A., Konishi, M., Ozaki, K., Fukui, S., and Itoh, N. (1998). Structure and expression of a novel fibroblast growth factor, FGF-17, preferentially expressed in the embryonic brain. Biochem. Biophys. Res. Commun. *244*, 187–191.

50. Brickman, Y.G., Ford, M.D., Gallagher, J.T., Nurcombe, V., Bartlett, P.F., and Turnbull, J.E. (1998). Structural modification of fibroblast growth factor-binding heparan sulfate at a determinative stage of neural development. J. Biol. Chem. *273*, 4350–4359.

51. Yabe, T., Hata, T., He, J., and Maeda, N. (2005). Developmental and regional expression of heparan sulfate sulfotransferase genes in the mouse brain. Glycobiology *15*, 982–993.

52. Ford-Perriss, M., Guimond, S.E., Greferath, U., Kita, M., Grobe, K., Habuchi, H., Kimata, K., Esko, J.D., Murphy, M., and Turnbull, J.E. (2002). Variant heparan sulfates synthesized in developing mouse brain differentially regulate FGF signaling. Glycobiology *12*, 721–727.

53. Nurcombe, V., Ford, M.D., Wildschut, J.A., and Bartlett, P.F. (1993). Developmental regulation of neural response to FGF-1 and FGF-2 by heparan sulfate proteoglycan. Science *260*, 103–106.

54. Hu, H. (2001). Cell-surface heparan sulfate is involved in the repulsive guidance activities of Slit2 protein. Nat. Neurosci. *4*, 695–701.

55. Skutella, T., and Nitsch, R. (2001). New molecules for hippocampal development. Trends Neurosci. *24*, 107–113.

56. Klein, R. (2004). Eph/ephrin signaling in morphogenesis, neural development and plasticity. Curr. Opin. Cell Biol. *16*, 580–589.

57. Raper, J.A. (2000). Semaphorins and their receptors in vertebrates and invertebrates. Curr. Opin. Neurobiol. *10*, 88–94.

58. Kantor, D.B., Chivatakarn, O., Peer, K.L., Oster, S.F., Inatani, M., Hansen, M.J., Flanagan, J.G., Yamaguchi, Y., Sretavan, D.W., Giger, R.J., and Kolodkin, A.L. (2004). Semaphorin 5A is a bifunctional axon guidance cue regulated by heparan and chondroitin sulfate proteoglycans. Neuron *44*, 961–975.

59. Pasquale, E.B. (2005). Eph receptor signalling casts a wide net on cell behaviour. Nat. Rev. Mol. Cell Biol. *6*, 462–475.

60. Bulow, H.E., and Hobert, O. (2004). Differential sulfations and epimerization define heparan sulfate specificity in nervous system development. Neuron *41*, 723–736.

61. Grobe, K., Inatani, M., Pallerla, S.R., Castagnola, J., Yamaguchi, Y., and Esko, J.D. (2005). Cerebral hypoplasia and craniofacial defects in mice lacking heparan sulfate *Ndst1* gene function. Development *132*, 3777–3786.

62. Irie, A., Yates, E.A., Turnbull, J.E., and Holt, C.E. (2002). Specific heparan sulfate structures involved in retinal axon targeting. Development *129*, 61–70.

63. Kinnunen, T., Huang, Z., Townsend, J., Gatdula, M.M., Brown, J.R., Esko, J.D., and Turnbull, J.E. (2005). Heparan 2-*O*-sulfotransferase, *hst-2*, is essential for normal cell migration in *Caenorhabditis elegans*. Proc. Natl. Acad. Sci. USA *102*, 1507–1512.

64. Deepa, S.S., Umehara, Y., Higashiyama, S., Itoh, N., and Sugahara, K. (2002). Specific molecular interactions of oversulfated chondroitin sulfate E with various heparin-binding growth factors. Implications as a physiological binding partner in the brain and other tissues. J. Biol. Chem. *277*, 43707–43716.

65. Chen, J.H., Wen, L., Dupuis, S., Wu, J.Y., and Rao, Y. (2001). The N-terminal leucine-rich regions in Slit are sufficient to repel olfactory bulb axons and subventricular zone neurons. J. Neurosci. *21*, 1548–1556.

66. Liu, G., Beggs, H., Jurgensen, C., Park, H.T., Tang, H., Gorski, J., Jones, K.R., Reichardt, L.F., Wu, J., and Rao, Y. (2004). Netrin requires focal adhesion kinase and Src family kinases for axon outgrowth and attraction. Nat. Neurosci. *7*, 1222–1232.

67. Taylor, K.A., and Buchanan-Smith, J.G. (1992). A colorimetric method for the quantitation of uronic acids and a specific assay for galacturonic acid. Anal. Biochem. *201*, 190–196.

68. Fan, C.M., and Tessier-Lavigne, M. (1994). Patterning of mammalian somites by surface ectoderm and notochord: evidence for sclerotome induction by a hedgehog homolog. Cell *79*, 1175–1186.

69. Ward, M.E., and Rao, Y. (2005). Investigations of neuronal migration in the central nervous system. Methods Mol. Biol. *294*, 137–156.

70. Zhu, Y., Li, H., Zhou, L., Wu, J.Y., and Rao, Y. (1999). Cellular and molecular guidance of GABAergic neuronal migration from an extracortical origin to the neocortex. Neuron *23*, 473–485.

